18th International Conference on Space Operations, Montreal, Canada, 26 - 30 May 2025.

SpaceOps-2025, ID 501

Flight Dynamics System for Space-Based Space Surveillance and Tracking

Mirko Trisolini[a]*, Andrea Carlo Morelli[a], Simon Van Hulle[a], Mario Carabellò[a], Asuthosh Ramesh[a], Alvaro Martinez Chamarro[a] , David Gondelach[a]

[a] *Vyoma GmbH, Munich, Germany*
* Corresponding Author, *mirko.trisolini@vyoma.space*

Abstract

This paper presents the development of Vyoma's in-house Flight Dynamics System. It focuses on introducing the capabilities of the system such as event prediction, orbit determination, manoeuvre optimisation, and conjunction assessment. The application of the system to enable Vyoma's pilot mission to perform space-based surveillance and tracking is highlighted. Following a description of the different building blocks of the Flight Dynamics System, a series of use cases are presented to demonstrate its capabilities. Finally, the integration of the Flight Dynamics System with Vyoma's Mission Planning System is presented and discussed.

Keywords: flight dynamics, mission planning, space sustainability, space situational awareness

Acronyms/Abbreviations

AEM	Attitude Ephemeris Message
CAM	Collision Avoidance Manoeuvre
CCSDS	Consultative Committee for Space Data Systems
CDM	Conjunction Data Message
FDS	Flight Dynamics System
LEO	Low-Earth Orbit
MPS	Mission Planning System
OCP	Optimal Control Problem
OD	Orbit Determination
OEM	Orbit Ephemeris Message
SP	Special Perturbations
TLE	Two-Line Element

1. Introduction

With thousands of satellites in orbit, which provide critical services like telecommunications, geolocation and meteorology, ensuring their safety and the long-term sustainability of the space environment is paramount. Knowledge of the orbits of all objects in space, and management of the trajectories of active spacecrafts, is necessary. To support these space traffic management and space situational awareness tasks, Vyoma is developing Europe's first sovereign space-based surveillance system, capable of mapping the majority of space objects in low-Earth orbit (LEO). The first satellite is equipped with an optical telescope for precise surveillance and tracking of satellites and debris. The observations acquired by the telescope is post-processed and utilised to catalogue objects in space. To support customers, for example for conjunction assessment, specific objects shall be observed, and the observations downlinked and processed with minimum latency. This requires accurate pointing and precise orbit determination of the satellite. In addition, the operational orbit needs to be acquired after launch and controlled for station keeping, collision avoidance, and end-of-life disposal. For this purpose, an in-house Fight Dynamics System (FDS), built on in-house astrodynamics libraries, was developed for the mission. The developed FDS is equipped with core capabilities such as orbit propagation for orbital and attitude products generation, orbit determination for accurate estimation of the satellite state, and event prediction to enable operations such as ground contact scheduling, on-board resource management, and target observation opportunities prediction. The FDS also includes the optimisation of manoeuvres that can be flexibly used during orbit acquisition, station keeping, collision avoidance, and end-of-life disposal mission phases. The developed FDS and astrodynamics libraries are also the workhorse of Vyoma's in-house Mission Planning System (MPS); leveraging such capabilities, the MPS, in synergy with other ground segment components, can perform automated operations, scheduling, and commanding activities. The future goal of the developed FDS system is, in fact, to fully support automated satellite operations for the Flamingo-1 mission and for other systems. In addition to automated usage, the FDS can also be used manually in case of critical operations.

The paper is structured as follows. Section 2 describes the system architecture and the design choices for the FDS; Section 3 details the different capabilities of the FDS and gives details on the implementation of each of its core modules. Section 4 demonstrates the usage of the FDS for relevant use cases such as orbit determination and trajectory optimisation. Section 5 discusses the interface between FDS and MPS and their use for Vyoma's pilot mission. Finally, Section 6 contains the conclusions and the discussions.

2. System Architecture

Vyoma's Flight Dynamics System (FDS) and astrodynamics libraries have been developed to support the operations of our pilot mission, Flamingo-1, and of the future satellites of Vyoma's constellation for space-based surveillance and tracking. As such, the FDS can support the main functions that allow ground system operators and flight dynamics engineers to determine the orbits of the satellites, control the satellite and plan mission operations. The capabilities of the FDS are also leveraged by the Vyoma Mission Planning System (MPS) [1] to enable the optimisation and verification of the scheduling activities for Vyoma's satellites. Vyoma's FDS is based on the open-source low-level flight dynamics library Orekit [2] and its underlying mathematics library Hipparchus [3]. The FDS consists of a core of astrodynamics libraries based in Java and an outer layer in Python which provides an interface for manual use by operators and flight dynamics engineers. A non-exhaustive list of functionalities of Orekit is provided below:

- High accuracy date and time, handling of many common time systems (UTC, TAI, UT1, TT, GPS, etc.)
- Reference frames handling: J2000, GCRF, ICRF, ITRF from 1998 to 2020 and intermediate frames (TOD, MOD, GTOD and TEME), topocentric, local orbital frames, etc.
- IERS Earth Orientation Parameters, of JPL DE 4xx ephemerides,
- Tropospheric and ionospheric models, geomagnetic fields (IGRF, WMM), geoid models
- Numerical propagation
  - Customizable force models: central attraction, higher-order gravity models, drag, solar radiation pressure, third-body attraction, etc.
  - Atmospheric models: DTM2000, JB2008, NRLMSISE00
  - State of the art ODE integrators
  - Jacobian computation
- Semi-analytical propagation model (DSST [4]) with customizable force models
- Taylor-algebra and automatic differentiation
- Orbit determination using batch least squares and Kalman filter
- Events handling during propagation (eclipse, node crossings, stations' visibility, dates, etc.)
- Several attitude evolution models available (nadir pointing, yaw compensation, yaw-steering, LOF aligned, etc.) and easy customisation
- Impulsive and continuous manoeuvre handling

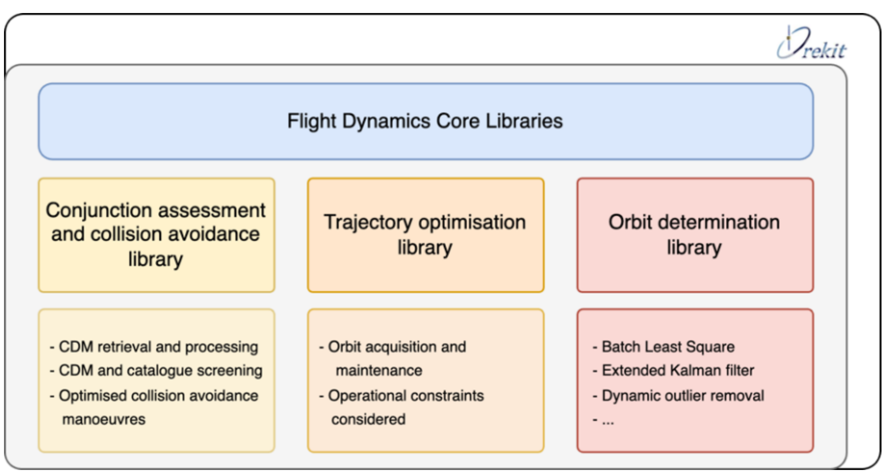

Fig. 1: Diagram of the FDS libraries architecture.

In addition to the previously listed functionalities provided by Orekit, the FDS is based on an in-house core astrodynamics library that contains the data models of the flight dynamics system and enhanced algorithms for orbit propagation and event prediction, as well as routines for the import, export and conversion of orbital and attitude data products (Fig. 1). Dedicated libraries have been developed for conjunction assessment and collision avoidance, trajectory optimisation, and orbit determination extending the core functionalities. The capabilities of these libraries are described in more detail in Section 3. This modularity allows for better integration of new functionalities and improvement of existing features without affecting the core FDS algorithms.

The FDS relates to other ground segment components and receives inputs from telemetry, such as GNSS data, and from spacecraft configuration data, such as the mass of the spacecraft and the characteristics of the thrusters (Fig. 2). Operational inputs can be passed to tailor the execution of specific actions to the operational scenario at hand. For example, the thresholds required do assess the criticality of conjunction events during a screening session. The Flight Dynamics System then generates products such as orbit predictions, attitude sequences, events predictions, and manoeuvre plans. These products can be analysed by an operator, who can manually interact with the FDS via a user interface. The products are also shared with the Mission Planning System, which uses them for the generation of the operations schedule of the spacecraft in the upcoming days, for example, scheduling ground station passes, payload operation sessions, TLE updates, and more.

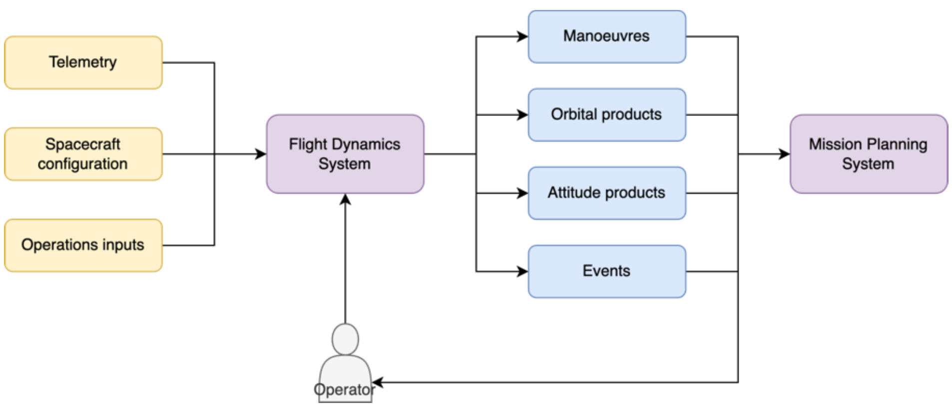

Fig. 2: Flow diagram with the main input and output interfaces of the FDS.

The main functionalities of the FDS are shown in Fig. 3:

- **Data Import and Conversions**: handles import of telemetry and orbit data in standardised formats (e.g., OEM, AEM, TLE)
- **Orbit Determination**: processes observations to accurately estimate the orbit of the spacecraft. Also manoeuvre calibration and estimation can be performed
- **Orbit Propagation**: uses the state estimated by the orbit determination to propagate and predict the future evolution of the spacecraft orbit and its covariance
- **Attitude Computation**: models the attitude evolution of the spacecraft and generates attitude sequences based on user-specified attitude modes
- **Event Prediction**: uses information generated by the orbit propagation and attitude computation modules to compute events such as eclipses and ground station passes
- **Conjunction Assessment**: routinely performs screening of the spacecraft operational orbit against CDMs and the catalogue to check for possible risky conjunctions
- **Manoeuvre Optimisation**: provides state-of-the-art algorithms for the optimisation of manoeuvres for collision avoidance, station keeping and orbit acquisition applications
- **Orbit Export and Product Generation**: collects the data results provided by the previously described modules and generates outputs in standardised formats and internal formats for the interaction of the FDS with other ground segments systems and external parties

3. Flight Dynamics System Capabilities

This chapter contains a more detailed description of the different functionalities and features of Vyoma's FDS. For each one of the main building blocks in Fig. 3, an overview of the available functionalities and details on their implementation is provided. In Section 4, selected use cases and examples of the capabilities of the FDS related to a selection of the functionalities described in the following are shown.

3.1. Orbit Propagation and Event Prediction

At the backbone of the functionalities of a flight dynamics system is the capability to accurately predict the evolution of the orbit of a spacecraft. This is usually achieved by integrating the equations of motion of the satellite as subject to external forces due to the gravity field of the Earth, the atmospheric drag, the solar radiation pressure, the manoeuvres the spacecraft performs, etc. Building on the core functionalities of Orekit, the FDS contains an Orbit Propagation module with the following characteristics:

- Propagate orbits via numerical propagation, Draper Semi-Analytical Satellite Theory (DSST) propagation [4] and SGP4 propagation theory [5]
- Propagation performed in Cartesian, Keplerian, and Equinoctial elements
- Customisable force models included in the propagation
    - Gravity field model using spherical harmonics with Earth Gravity Model 2008 (EGM-08)
    - Third-body perturbations of Sun, Moon, Jupiter and other planets
    - Atmospheric drag modelled as cannon ball with atmospheric model type selected among NRLMSISE00 [6] and DTM2000 [8]
    - Solar radiation pressure following a cannon ball approximation
    - Solid Earth Tides and post-Newtonian correction
- User-defined manoeuvre sequences both for impulsive and continuous thrust manoeuvres
- User-defined attitude sequences with predefined and customisable attitude modes
- Customisable spacecraft definition with initial state as Cartesian, Keplerian, Equinoctial or TLE state
- Covariance matrix propagation

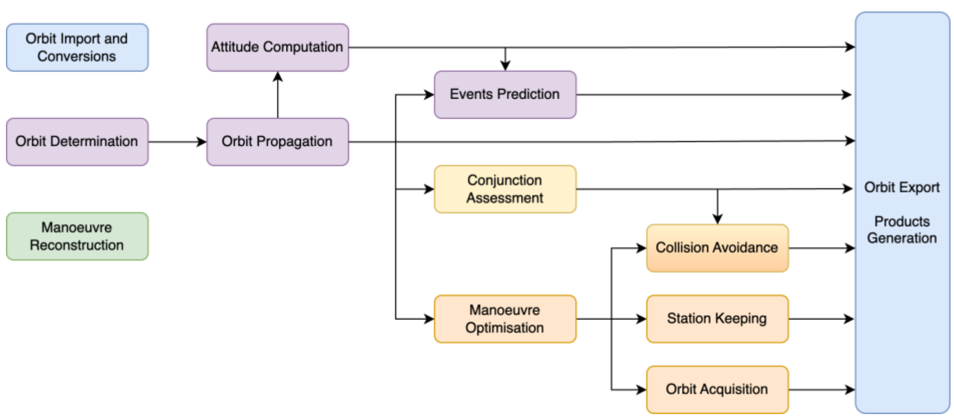

Fig. 3: Detail of the FDS modules and the connection among them.

Several options are available for the attitude sequence generation, depending on the desired attitude mode. The attitude modes currently supported by the FDS are:

- Nadir Pointing with Yaw Compensation: satellite z-axis is pointing to the vertical of the ground point under satellite
- Centre Pointing with Yaw Compensation: body centre pointing with yaw compensation
- Aligned with Local Orbital Frames (e.g. LVLH, QSW, TNW, VNC, etc.)
- Ground Station Pointing: spacecraft z-axis pointing towards the provided ground station
- Sun Pointing: the spacecraft points a body axis towards the Sun
- Thrust Aligned: the attitude of the spacecraft is such that the thruster points in the desired thrust direction
- Custom Orientation: user defined orientation

- Space Object Tracking: the attitude of the spacecraft is such that a body direction (e.g., payload boresight) points towards a target spacecraft, whose orbit can be defined by TLE or Keplerian parameters

The Space Object Tracking mode is of particular importance as it allows the Flamingo-1 satellite to track specific assets in space to perform dedicated observations.

The orbit and attitude propagated via the Orbit Propagation module are the fundamental information for the Event Prediction module of the FDS. The following are the events supported by the FDS:

- Eclipses, including or excluding penumbra
- Ground station link, with customisable ground station minimum elevation
- South Atlantic Anomaly passage
- Perigee and apogee crossing
- Ascending and descending node crossing
- Passage over Polar Horns
- Sun-Station-Satellite collinearity with customisable proximity angle
- Sensor blinding by the Sun, Moon, or Earth
- Ground station visibility opportunities from satellite sensor (e.g., an antenna requiring precise pointing for downlink)

3.2. Orbit Determination

When new measurements are received, the Orbit Determination (OD) module of the FDS is used to obtain an accurate estimate of the satellite's orbit. In the context of the Flamingo-1 mission, accurate satellite ephemeris is required for processing the observations of the telescope. At the same time, reliable orbit predictions form the basis of conjunction assessment and collision avoidance procedures (see Fig. 3).

The OD module allows for estimation of the spacecraft state, as well as dynamical parameters like the drag coefficient or reflection coefficient used in the force models for drag and solar radiation pressure perturbations. This can either be achieved using a batch least squares (BLS) optimisation or a sequential (extended/unscented Kalman filter) approach.

Using BLS, the OD module also enables several additional features:

- Estimating measurement parameters like observer clock biases.
- Estimating multiple values of dynamic parameters, e.g. one drag coefficient per day. This mostly serves to absorb inaccuracies of the dynamical model and avoids growing errors towards the ends of the fit span.
- Estimating the magnitude and direction of manoeuvres. This is used to identify systematic thruster errors that can feed back into the operations of the satellite.

For more accurate past ephemeris, a sequential approach can be more desirable since the errors are less dependent on the choice of measurement fit span. This, however, introduces the problem that the filter solution is not inherently continuous and smooth. The FDS has several capabilities to improve the Kalman filter estimation results:

- Time-dependent process noise, tuned for different altitude regimes and for the specific dynamical model of choice by comparing orbit predictions with reference ephemeris.
- Rauch-Tung-Striebel (RTS) smoothing [9] to backward smooth the filter estimates after processing all available measurements. This results in a smooth and more accurate orbit ephemeris and reduces large errors due to measurement gaps.
- Orbit blending [10] with analytical or numerical propagation to obtain a continuous ephemeris that is reliable in the presence of measurement gaps.

A selection of the mentioned capabilities is demonstrated by relevant examples in Section 4.1.

3.3. Manoeuvre optimisation

Another core functionality of Vyoma's FDS is the trajectory optimisation suite. It is a powerful tool capable of handling optimisation problems for collision avoidance, station keeping, and transfer trajectory manoeuvre computation that relies on algorithms fully developed in-house. The company's algorithms are based on convex optimisation methods [15] and are able to consider both low- and high-thrust propulsion systems. The convex optimisation approach has been selected due to its very low computational burden, high convergence rate, and versatility [17], and represents the state-of-the-art in terms of space trajectory optimisation. It has recently been applied to various space-based applications, including collision avoidance [19] and low-thrust trajectory optimisation [18], and for the autonomous landing of SpaceX's Falcon 9 [21].

The spacecraft manoeuvre optimisation suite of Vyoma's FDS solves optimal control problems (OCP) of the form:

$$\begin{aligned} \text{minimise} \quad & f(\boldsymbol{x}, \boldsymbol{u}) \\ \text{subject to} \quad & \boldsymbol{g}(\boldsymbol{x}, \boldsymbol{u}) \leq \boldsymbol{0} \\ & \boldsymbol{h}(\boldsymbol{x}, \boldsymbol{u}) = \boldsymbol{0}, \end{aligned} \tag{1}$$

where $\boldsymbol{x}$ and $\boldsymbol{u}$ are the state and control variables of the spacecraft, respectively; $f(\boldsymbol{x}, \boldsymbol{u})$, is the objective function of the problem, which corresponds to the spacecraft's fuel consumption. The inequality constraints, $\boldsymbol{g}(\boldsymbol{x}, \boldsymbol{u}) \leq \boldsymbol{0}$, include e.g. the variables bound, whereas the equality constraints, $\boldsymbol{h}(\boldsymbol{x}, \boldsymbol{u}) = \boldsymbol{0},$ include e.g. the dynamical constraints and the initial and possibly final boundary conditions. On top of that, several operational constraints are modelled as mathematical equations and included in the OCP. A summary of the considered operational constraints is as follows:

- Require free, tangential, or constant thrust direction in local reference frame (RTN) for each thrust arc.
- In case of collision avoidance, consider multiple conjunctions in the same optimisation.
- In case of collision avoidance, impose the return to the nominal orbit after the collision avoidance manoeuvre (CAM) is executed.
- Impose duty cycles when the engines must be switched off for some time periods during the optimisation time horizon.
- Require thrust off during eclipses.
- Impose a minimum thrust arc duration.

The trajectory optimisation can be performed in Cartesian, Keplerian, or Modified Equinoctial Elements coordinates, and the spacecraft dynamical model can consider two-body acceleration, J_2 effect, and drag.

The resulting OCP is solved through a methodology called Sequential Convex Programming (SCP) [20]. The idea behind SCP is that the original nonconvex OCP is approximated as a convex problem; a series of convex subproblem instances is solved iteratively until the series of solutions to these subproblems eventually converge to the solution of the original nonconvex problem. Fig. 4 summarises the SCP algorithm logic, which consists of the following steps:

1. Formulate the full nonconvex optimisation problem.
2. By means of different convexification techniques, such as lossless convexification or linearisation [17], formulate the correspondent convex sub-problem.
3. Transform the continuous-time convex problem into a discrete one by means of a collocation method [22].
4. Build the problem to be solved by specifying the reference solution about which the problem is linearized.
5. Solve the problem by means of a convex solver.
6. Check whether the nonconvex constraints are respected according to some criteria or up to a user-selected threshold; if so, go to the following step. Otherwise, go to step 4.
7. The solution of the original nonconvex problem is obtained.

As highlighted in Step 3 of the SCP algorithm overview, convex optimisation is a collocation approach, which means that the solution of the problem in terms of optimal control variables is only given as specific points in time. Operatively speaking, this represents a strong limitation as thrust commands to be sent to the spacecraft are usually described in terms of start epoch, duration, and thrust direction expressed in a specific reference frame (e.g., inertial or local). For the Vyoma's manoeuvre optimisation software suite to fully support the generation of operational manoeuvre commands, a post-processing procedure has been developed and implemented, which is referred to as thrust regularisation [24]. It refers to the transformation of the raw control output of the SCP algorithm into a thrust profiles where each thrust arc is defined by the start epoch, duration, and thrust direction only.

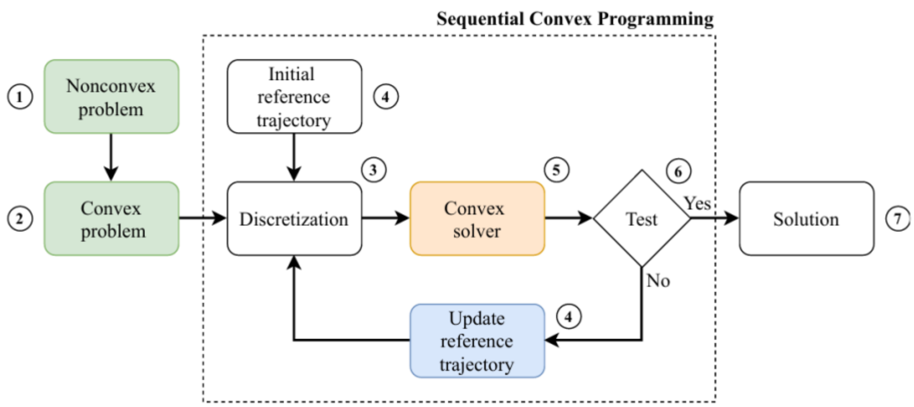

Fig. 4: SCP algorithm logic (figure from [7]).

3.3.1. Orbit transfer optimisation

Especially in the case of low-thrust propulsion systems, orbit transfers can be long and last several days, weeks, or even months. If the SCP algorithm is used directly for such cases, the collocation nature of convex optimisation necessitates the usage of a rather large amount of discretisation nodes (usually, for LEO mission, 1 node is used every 60 seconds [19]). This would result in very high computational times and would basically nullify the advantages of convex optimisation.

Therefore, to deal with long transfer times, Vyoma's orbit transfer optimisation activity is performed using a Model Predictive Control (MPC)-like approach [16]:

1. First, a reference trajectory for the whole transfer is found using an in-house-developed Lyapunov-based Q-law algorithm [26].
2. The SCP algorithm is used to compute the operationally compliant thrust profile for shorter time horizons (e.g., few days); this is basically a refinement of the reference trajectory found at step 1, where operational constraints are imposed.
3. During spacecraft operations, an orbit determination process is performed periodically; the difference of the spacecraft state with respect to the reference trajectory is evaluated and, if necessary, a new reference trajectory is computed.
4. The process is iterated for the whole transfer.

The workflow of Steps 1 and 2 is detailed in Fig. 5. Step 2 is not performed through one single optimisation. Both the reference trajectory obtained at Step 1 and the SCP optimisation of Step 2 are obtained using simplified dynamical models; therefore, it is necessary to introduce higher-fidelity dynamics to obtain an operationally compliant thrust profile. Since including high-fidelity dynamics would make the optimisation of the Q-Law and SCP algorithms cumbersome, the convex optimisation refinement is performed in multiple steps. The full SCP optimisation of Step 2 is subdivided into shorter sub-problems; for each sub-problem, the SCP is solved to target the reference Q-Law trajectory. Once the SCP problem is solved and the thrust profile is found for a sub-problem, a high-fidelity propagation is performed to account for more accurate dynamics. This allows the computation of the final state of the sub-problem, which then becomes the initial state of the following sub-problem, which is solved in the same fashion until the last sub-problem that comprises the whole time-span of Step 2 is reached.

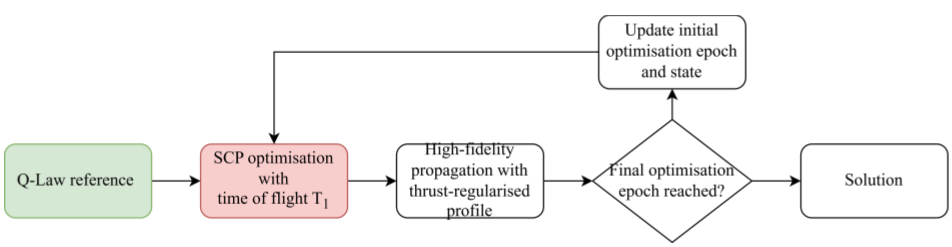

Fig. 5: Detailed procedure for operational orbit acquisition through Vyoma's FDS Toolkit.

3.4. Conjunction Assessment and Collision Avoidance

Vyoma's FDS also includes conjunction assessment and collision avoidance capabilities. The system is fully integrated with SpaceTrack* to retrieve the latest Conjunction Data Messages (CDMs) generated by the US 18th Space Defence Squadron. Additionally, the FDS updates existing CDMs when more accurate orbit or spacecraft information is available for the primary and/or secondary object. Independent CDMs can also be generated when orbit and covariance information is available for both the primary and the secondary.

Screening capabilities are available to detect potentially high-risk conjunctions. A user provided ephemeris can be screened against upcoming CDMs or against all catalogued objects using the SP ephemeris of catalogued objects. This enables users to assess if planned trajectories, e.g. planned manoeuvres, are safe.

Alongside the screening capabilities, Vyoma's FDS is also capable of computing and planning collision avoidance manoeuvres. These manoeuvres are generated using the in-house optimisation algorithm as described in Section 3.3, which is capable of dealing with both chemical and electric propulsion systems, as well as differential drag manoeuvres, and is able to integrate several mission constraints directly into the manoeuvre design, thus avoiding overheads in the computation and planning of collision avoidance manoeuvres. This is of utmost importance when considering the increasing space traffic and conjunction events and the unavoidable need for automation of such procedures. Relying on an optimal, fast, and reliable algorithm for collision avoidance is a key aspect of Vyoma's FDS suite.

3.5. Data Export and Products Generation

Vyoma's FDS uses JSON files as internal format to standardise the information exchange between the different modules of the FDS. For external interfaces, the FDS supports standardised formats of the Consultative Committee for Space Data Systems (CCSDS) [11] via parsing and creation of the following formats:

- Orbit Ephemeris Messages (OEMs)
- Orbit Parameter Messages (OPMs)
- Orbital Mean-Elements Messages (OMMs)
- Attitude Ephemeris Messages (AEMs)
- Conjunction Data Messages (CDMs)
- Tracking Data Messages (TDMs)

The FDS also supports other specialised data formats such as Two-Line Elements (TLEs), Special Perturbation (SP) Ephemeris, Standard Product 3 (SP3) orbit data, and the Consolidated Prediction Format (CPF).

Vyoma's FDS is therefore fully capable to interact with external systems and other entities and share relevant information via the commonly supported data formats in the space sector.

4. Use cases

The following sections show some relevant examples of the capabilities of Vyoma's FDS with focus on two core functionalities of the system: orbit determination and manoeuvre optimisation. Section 4.1 presents a manoeuvre calibration case using orbit determination as well as an example of smoothing for orbit estimation. Section 4.2 shows examples of manoeuvre optimisation for collision avoidance and station keeping.

4.1. Orbit determination

Two examples are discussed to showcase the capabilities of the OD module of the FDS. The first example uses position measurements to calibrate a known manoeuvre, and the second demonstrates the value of filtering and smoothing to obtain accurate ephemeris in case of large uncertainties in the dynamical model.

4.1.1. Manoeuvre Calibration

One of the OD capabilities is calibrating the parameters of a known manoeuvre to improve the measurement fit and orbit prediction. To illustrate this, the Sentinel-2A satellite (780 km altitude) is considered around the time of a reported manoeuvre in June 2024. Table 1 shows the details of the manoeuvre, as reported by ESA†.

---

* https://www.space-track.org

Table 1: Reported constant thrust manoeuvre for Sentinel-2A†

Parameter	Value
Start epoch	2024/06/27 at 15:53:23.716 UTC
Thrust duration	10.624 s
Acceleration vector (RTN)	[-0.24360105e-8; 0.20990374e-5; 0.0] m/s²
Thrust magnitude	2.313 N
Spacecraft mass	1101.950 kg

The ESA precise ephemeris is used as the ground truth for simulating observations and comparing estimation results. Position measurements are simulated in a 1-day window around the manoeuvre by adding Gaussian noise with $\sigma = 3$m to each of the Cartesian position coordinates of the ground truth, sampled once per minute. Using a dynamical model that includes 48x48 spherical harmonic gravity, drag, solar radiation pressure and third body perturbations from the Sun and Moon, the orbit is estimated along with the ballistic and radiation pressure coefficients. The quality of the estimation is then evaluated by comparing the propagated orbit with the ground truth. Two different estimation setups are considered:

- Without manoeuvre calibration: the reported manoeuvre is assumed perfectly accurate.
- With manoeuvre calibration: the thrust magnitude and direction of the manoeuvre are estimated during the orbit determination.

Fig. 6 shows the errors compared to the ground truth after BLS OD with both setups. Inside the measurement fit span, without manoeuvre calibration the errors are largest at the epoch of the manoeuvre, see red curve. This effect is eliminated when estimating the manoeuvre magnitude and direction, see blue curve. The resulting prediction errors are reduced by more than an order of magnitude after 1 day of propagation when calibrating the manoeuvre.

The estimation results with both setups are compared in Table 2. The distribution of the residuals with manoeuvre calibration matches the artificial measurement noise, which indicates a good fit. The thrust magnitude is calibrated at 98.3% of the reported value and the thrust direction is adjusted by –0.24 deg in azimuth and –1.3 deg in elevation. Note that these adjustments do not necessarily reflect pure errors in the reported manoeuvre but can also absorb uncertainties in the chosen dynamical model. However, by continuously estimating the thrust parameters for the same satellite, the OD module can be used to identify uncertainties and systematic offsets between planned and observed manoeuvres. This example shows the importance of manoeuvre calibration and demonstrates how the FDS can be used provide accurate orbit predictions for operational use.

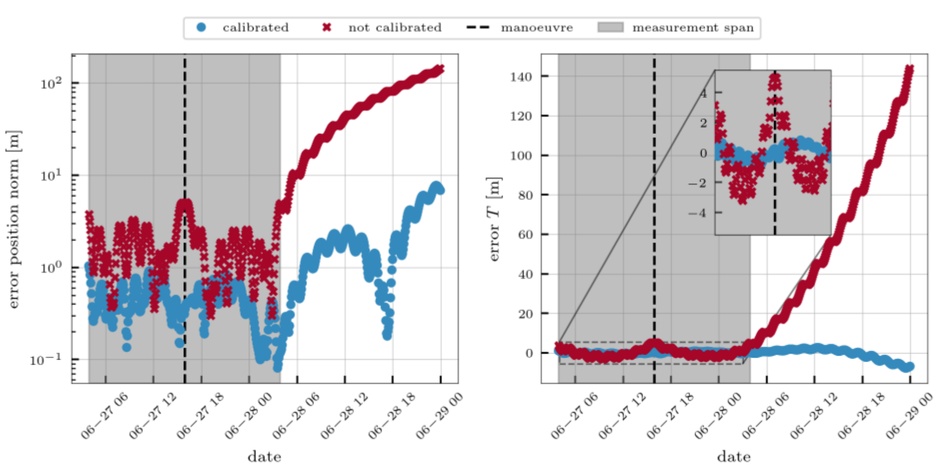

Fig. 6: Estimation errors for Sentinel-2A compared to ESA precise ephemeris for cases with and without calibrating the manoeuvre parameters. Left: norm of the position error, right: position error in along-track direction (T).

† https://sentiwiki.copernicus.eu/web/s2-processing

Table 2: Orbit determination results for Sentinel-2A with and without manoeuvre calibration.

Parameter	Without manoeuvre calibration	With manoeuvre calibration
Normalised measurement residual RMS	1.08	1.00
4-day predicted position error	1975 m	75.1 m
Estimated Ballistic coefficient	0.028 m²/kg	0.017 m²/kg
Estimated SRP coefficient	0.014 m²/kg	0.012 m²/kg
Estimated thrust magnitude	(2.313 N)	2.273 N
Estimated azimuth offset (RTN)	(0.0)	−0.24 deg
Estimated elevation offset (RTN)	(0.0)	−1.3 deg

4.1.2. Sequential estimation

The second OD example illustrates the benefit of sequential estimation using filtering and smoothing to achieve accurate orbit estimates in case of larger uncertainties in the dynamical model. Here, the ground truth is the SP3 ephemeris of the SWARM-A satellite (~450 km altitude) in November 2024[‡]. Since this time corresponds to a solar maximum, the drag is high and the limited accuracy in the NRLMSISE-00 model causes significant propagation errors. Position measurements are again generated by adding artificial Gaussian noise to the precise ephemeris, this time with $\sigma = 8$m in each direction. Using the same dynamical model as in the previous example, the orbit is estimated over two days using four different approaches:

- BLS with single BC: First, Batch Least Squares is used, estimating a single value for the ballistic coefficient (BC) along with the orbital parameters and SRP coefficient. As expected, this results in large post-fit errors, predominantly in the along-track direction due to inaccuracies in the atmospheric density model, see Fig. 7.
- BLS with multiple BC: To improve the fit while keeping a smooth orbit solution, multiple values of the BC are estimated to compensate for time-varying errors in the density model. Using one BC value per 12 hours significantly reduces the maximum error, see Fig. 7. Still, the estimated orbit is less accurate than the measurements in the fit span, see Table 3.
- EKF: Adopting a sequential approach with an extended Kalman filter (EKF) strongly reduces the orbit error as the filter can deal with uncertainties in the dynamical model. Still, the filter solution contains discontinuous jumps at measurement epochs, particularly at the beginning of the fit span, see Fig. 7.
- EKF + Smoother: Applying RTS smoothing after the Kalman filter removes unwanted jumps and further reduces the position error RMS to 6.2 times below the RMS of the measurement error, see Table 3.

Table 3: SWARM-A estimation error RMS for different estimation approaches.

Method	Position error RMS
Measurements	13.9 m
Batch LS with constant ballistic coefficient	109 m
Batch LS with 12-hour ballistic coefficient	14.8 m
EKF	3.78 m
EKF + Smoother	2.23 m

Table 3 summarises the post-fit estimation error RMS for each of these OD approaches as compared to the precise ephemeris from which the measurements were derived. Fig. 7 shows the time-evolution of the along-track estimation error, as this component dominates the overall errors. Note that the improvement that can be achieved with a filter and smoother are highly dependent on the choice of fit span, observation noise distribution, orbit altitude and solar activity, but the smoother generally results in large error reductions in case of high drag or other large dynamical uncertainties.

[‡] https://swarm-diss.eo.esa.int/#swarm%2FLevel2daily%2FEntire_mission_data%2FPOD%2FRD%2FSat_A

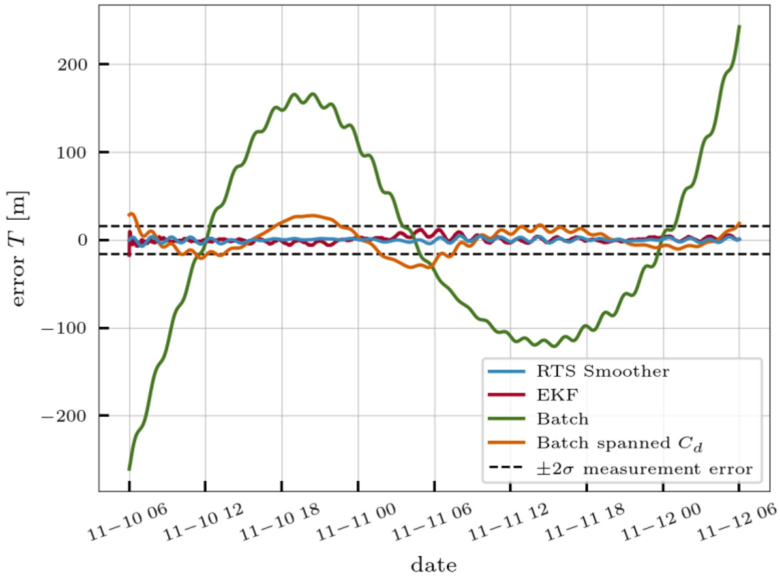

Fig. 7: Estimation errors for SWARM-A compared to precise ephemeris in along-track direction.

4.2. Manoeuvre Optimisation

In this section, three different test cases are presented to highlight the capability and flexibility of Vyoma's trajectory optimisation tool. Section 4.2.1 shows the results for a collision avoidance manoeuvre optimisation including operational constraints and considering both high- and low-thrust engines. Section 4.2.2.2 shows an orbit transfer with several days of manoeuvres.

4.2.1. Collision avoidance manoeuvre optimisation

To show Vyoma's FDS capabilities in terms of collision avoidance manoeuvre optimisation, the following scenarios are considered:

- **Scenario 1**: a satellite equipped with low-thrust propulsion must perform a collision avoidance manoeuvre to increase the miss distance associated with two conjunctions that take place approximately 4 hours apart; the satellite also needs to return back to its nominal orbit after the second conjunction. It is required that the thrust arcs have a constant direction in the local radial, transverse and normal (RTN) reference frame. Finally, eclipses are present during which the thrust must be zero.
- **Scenario 2**: a satellite equipped with a high-thrust propulsion system must perform a collision avoidance manoeuvre to decrease the probability of collision for one conjunction. It is required that the thrust is tangential. Eclipses are also present in this case.

Table 4 summarizes the thrusters characteristics for the two scenarios. For both cases, the optimisation is performed in Cartesian coordinates and considers a dynamical model that includes two-body acceleration and the J_2 perturbation.

Table 4: Thrusters characteristics for collision avoidance scenarios.

	Scenario 1	Scenario 2
T_{max} [N]	0.1	0.73
I_{sp} [s]	1600	300
m_0 [kg]	300	2150

Scenario 1

The first scenario involves two fictitious conjunction events happening respectively on 2025-03-30 at 03:30:47.230 UTC and 2025-03-30 at 07:34:32.769 UTC. The orbital parameters of the primary at the first TCA are reported in Table 5.

Table 5: Primary object orbital parameters at first TCA for Scenario 1 in EME2000.

Parameter	Value
Semi-major axis [km]	6927.13
Eccentricity [-]	0.00035
Inclination [deg]	97.59
RAAN [deg]	34.55
Argument of perigee [deg]	-53.91
True anomaly [deg]	-113.03

The miss distances of the two events are 799.58 m and 1630.15 m, respectively. A series of manoeuvres must be designed such that the miss distance of the two events is greater or equal than 2000 m. The manoeuvres can start 0.8 orbits before the first TCA, and the spacecraft must return to the nominal orbit within the 0.8 orbits after the second TCA. This is because typical CAMs are executed 0.5 orbits before TCA, and some margin was considered for the optimiser to have a larger solution set. Fig. 8 presents the thrust profile obtained by the SCP optimizer. The x-axis indicates the time from the first TCA in hours; The y-axis indicates the thrust control action (i.e., the normalised thrust). The plot shows the thrust magnitude, the thrust direction in RTN reference frame, and the eclipses. The most relevant characteristics of the profile are:

- It consists of 6 thrust arcs.
- The profile is bang-off-bang, meaning that the thrust is either on at its maximum value or off. This is an indication that a (near-)optimal solution has been found by the algorithm [25].
- The thrust direction is constant for each thrust arc in RTN reference frame.
- Contrary to what is often executed in case of CAMs [23], the optimal thrust direction is non-tangential for several thrust arcs. This is because the considered example is quite more complex than the typical scenario where only one conjunction is considered without any operational constraints. Therefore, in this case, it is likely that the fuel-optimal solution is not necessarily tangential.
- Two arcs are performed before the first conjunction to match the required minimum miss distance for the first event; two more thrust arcs are performed between the two conjunctions to match the required minimum miss distance for the second event; two additional manoeuvres bring the spacecraft back to the nominal orbit.

It is worth noting that such complex series of manoeuvres were found by the SCP algorithm in six iterations, for a total convex solver time of only 2.37 seconds on a 13th Gen Intel(R) Core (TM) i7-13700H 2.40 GHz with 32GB RAM.

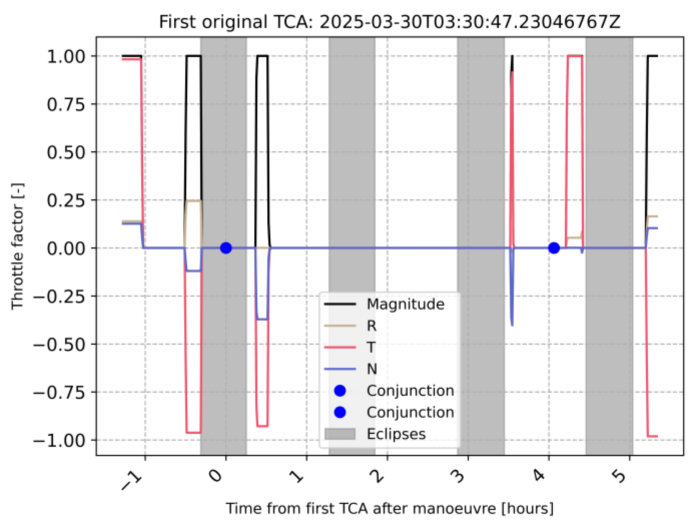

Fig. 8: Non-regularized thrust profile for Scenario 1.

Fig. 9 shows the difference between the nominal primary orbit and the post-manoeuvre orbit in terms of orbital parameters (semi-major axis, eccentricity and inclination). Note that the two orbits have been obtained by propagating the spacecraft dynamics with a *high-fidelity* dynamical model that includes a 48x48 gravitational model, perturbations from the Sun and Moon, drag, solar radiation pressure, and relativity effects. The post-manoeuvre orbit propagation has been performed using the regularised thrust arcs found by the SCP algorithm. It can be noticed that the series of manoeuvres result in a semi-major axis change of maximum 500 m. Still, after the last thrust arc, the difference reduces as expected to approximately zero.

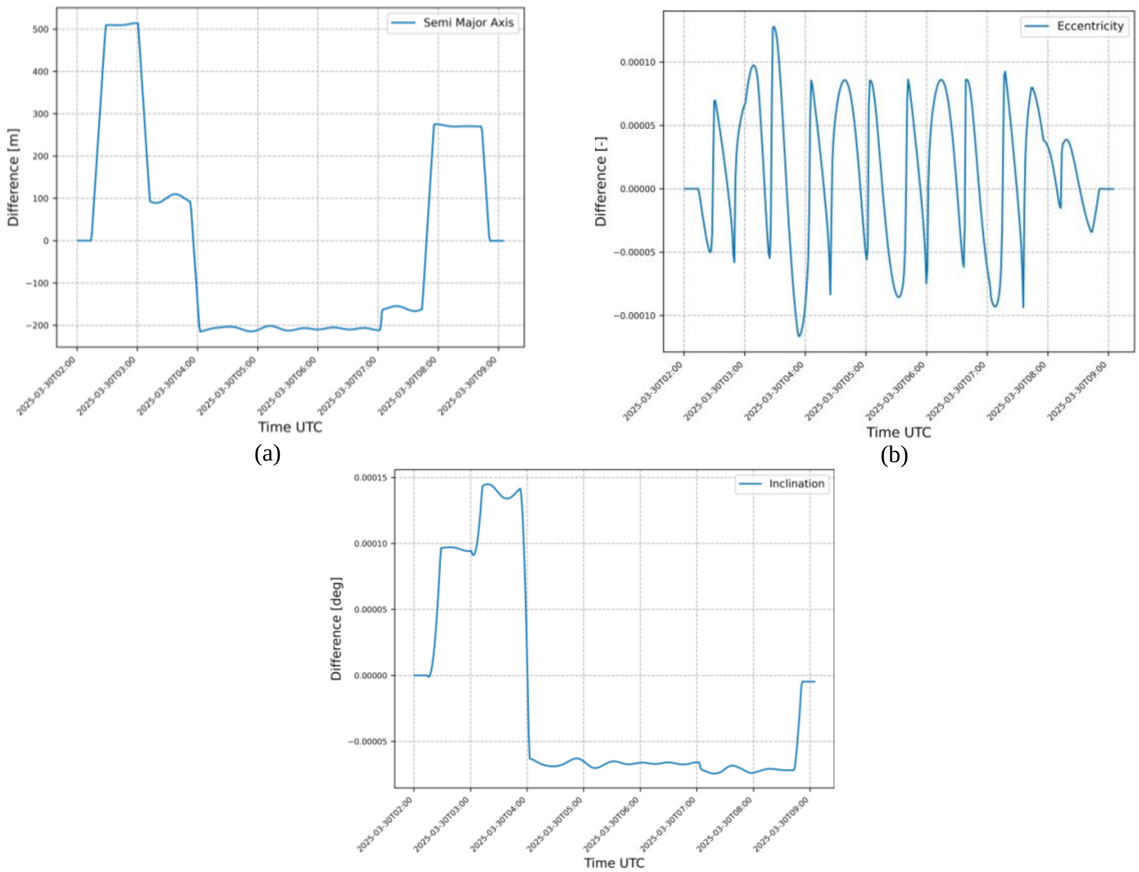

(a) (b) (c)

Fig. 9: Pre- and post- manoeuvre differences for (a) semi-major axis, (b) eccentricity, and (c) inclination for Scenario 1.

Scenario 2

The second scenario involves one fictitious conjunction event happening on 2025-04-14 at 02:35:09.818 UTC. The orbital parameters of the primary at the first TCA are reported in Table 6.

Table 6: Primary object orbital parameters at TCA for Scenario 2 in EME2000.

Parameter	Value
Semi-major axis [km]	6921.03
Eccentricity [-]	0.00018
Inclination [deg]	97.60
RAAN [deg]	36.47
Argument of perigee [deg]	93.27
True anomaly [deg]	-60.18

The probability of collision for this conjunction is $2.22569 \cdot 10^{-5}$, and a CAM should be designed to bring such probability to a safer value of $1.0 \cdot 10^{-6}$. In this case, the manoeuvres can start 2 orbits before TCA. Fig. 10a shows the obtained thrust profiles in case eclipses are not considered, while Fig. 10b shows the thrust profiles when eclipses are considered. It is interesting to notice that in case eclipses are neglected, the thrust burns happen approximately 0.8 and 2.4 hours before TCA. Since the orbital period of the primary object is approximately 1.6 hours, this means that the burns are centred at 0.5 and 1.5 primary orbits before TCA. This is consistent with what literature shows: optimal CAMs that decrease the probability of collision should be performed 0.5*n* (*n* integer) orbits before TCA [19]. When eclipses are considered, both thrust burns are shifted to avoid the eclipse windows, which overlap with the original, unconstrained thrust arcs.

The case without eclipses converged in three SCP iterations and with a remarkable total solver time of 0.26 seconds on the same machine as per the previous case. The computational time for Scenario 2 is significantly lower with respect to the computational time for Scenario 1 because fewer operational constraints were imposed, and the optimisation time horizon was significantly shorter.

Usually, collision avoidance manoeuvres are performed with tangential thrust. However, the optimal thrust direction of CAMs is not always tangential [19]. In a space environment where more and more conjunction events are happening due to the increase of the number of satellites in orbit, saving fuel becomes paramount. Table 7 shows the fuel mass consumption for Scenario 2 with eclipses for different requirements on the thrust direction. From the table it is interesting to see that if a constant thrust direction in the RTN frame is required (as per Scenario 1), the fuel mass consumption is the same as per the free thrust direction case. This might be because the optimisation algorithm is capable of finding alternative solutions that still minimise the fuel consumption. In case of tangential thrust, however, the required propellant mass increases by 2.4g (~3% more than in the unconstrained case).

Table 7: Fuel mass consumption for Scenario 2 and different constraints on the thrust direction.

	Free	Constant in RTN	Tangential
Δm [g]	85.1	85.1	87.5

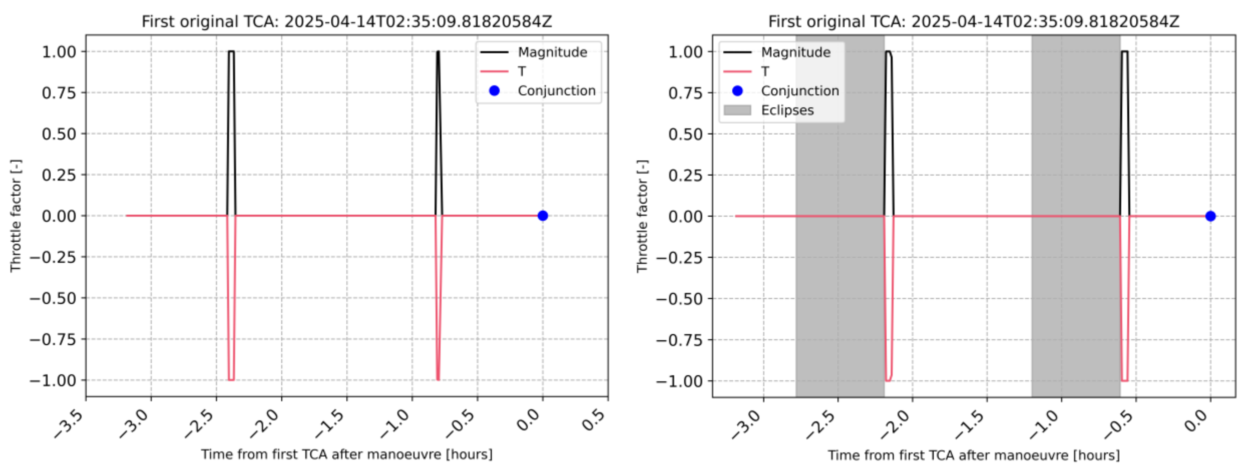

(a) (b)

Fig. 10: Thrust profiles for collision avoidance manoeuvre Scenario 2. (a) without eclipses and (b) with eclipses.

4.2.2. Orbit transfer optimisation

To demonstrate the FDS capabilities in terms of transfer trajectory design and optimisation, an example is shown where both the Q-Law and the convex trajectory optimiser are exploited. The test case presents a LEO-to-LEO transfer where the spacecraft semi-major axis and inclination are required to change. In particular, the semi-major axis change is approximately 80km, whereas the inclination change is approximately 0.25 degrees. First, a reference trajectory is found using the Q-Law algorithm. Then, the control commands for the first 72 hours of the transfer are refined using the convex optimiser, with a time of flight of 6 hours for each optimisation (see Fig. 5). In the refinement step, several operational constraints are included. Table 8 summarises the operational and dynamical constraints included in the Q-Law and in the convex optimiser. The *duty cycle constraints* mentioned in the table indicate the imposition of forced coast periods. In real operations, coast periods may be required for different reasons, such as ground station passes or batteries recharge that require a specific spacecraft attitude. The example presented here considers 30 minutes of forced coast arc period and every period where thrust arcs are admitted. The high-fidelity propagation in between each SCP optimisation (see Fig. 5) includes a 48x48 gravity model, Sun and Moon third-body perturbations, drag, solid earth tides, solar radiation pressure, and relativity effects.

Table 8: Data of the operational orbit acquisition example.

	Q-Law	Convex optimiser
Thrust direction constraints	No	Constant RTN
Min. thrust arc duration	No	5 minutes
Duty cycle constraints	No	Yes
One thrust arc per thrust free period	No	Yes
J_2 perturbation	Yes	Yes
Drag perturbation	Yes	Yes

Since the objective of the manoeuvre design is to change the semi-major axis and the inclination of the spacecraft, the other orbital parameters are not included in the final boundary conditions of the convex optimiser.
The whole procedure took 8.75 minutes to converge, which is remarkable given the numerous operational constraints imposed. Fig. 11 shows the thrust profile that comes out of the convex optimiser. As required, each of the thrust arcs has a constant direction in RTN reference frame (where the tangential and normal components are predominant because of the required change in semi-major axis and inclination). To make the profile operationally executable, the thrust arcs are then regularised and each of them is described by the start epoch, duration, and constant direction in RTN.
In this way, the FDS is able to obtain optimal manoeuvres that can be commanded to the satellite to perform orbit acquisition, station keeping, or end-of-life disposal.

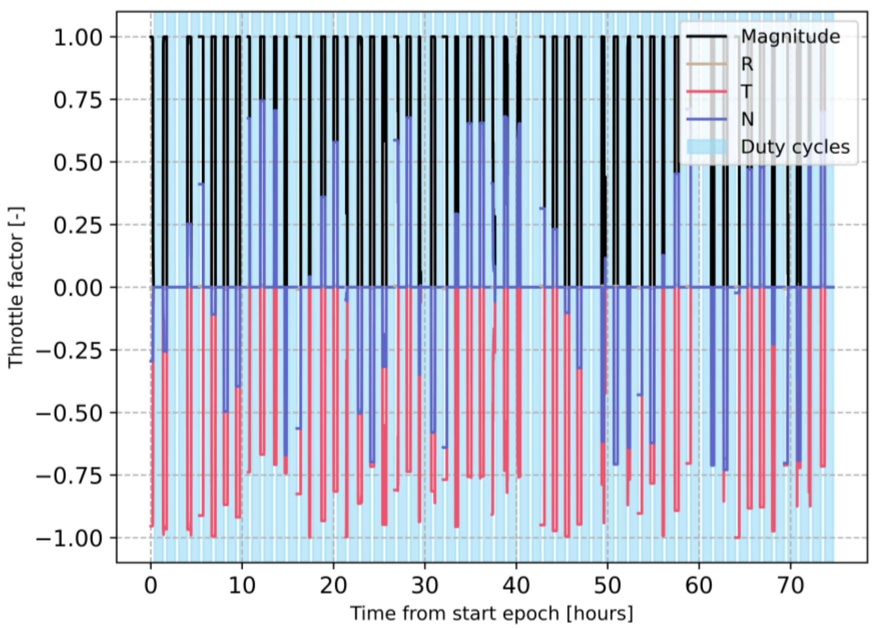

Fig. 11: Thrust profile for the orbital change test case obtained with convex optimisation.

5. Integration with Mission Planning System

Vyoma's in-house developed mission planning system (MPS) strongly relies on the FDS. The MPS is a complex tool dedicated to scheduling the activities of satellites and constellations following the mission and satellite requirements. It handles the different resources of the spacecraft and the requirements from the payload to organise and prioritise the activities automatically over a specified time horizon by optimising the mission objective and the resource usage. It is also connected to the mission control system to generate the commands for the spacecraft to perform the scheduled activities. The MPS is coupled with the FDS because it uses many FDS features to make informed decisions during the scheduling and related activities. For example, it uses the event prediction capabilities of the FDS to identify the upcoming ground passes and schedule contacts with the ground station, it uses the orbit and attitude propagation capabilities of the FDS to schedule tracking of other satellites and perform dedicated observation. All these activities are powered by the interaction between Vyoma's FDS and MPS. Nevertheless, the MPS can also interface with other flight dynamics systems as it relies on generic interfaces.

Fig. 12 shows a snapshot of the mission planning system interface. The figure shows at the top the scheduled activities such as ground station contacts, satellite health checks, manoeuvres, and other actions. In the middle, one can see the utilisation of one of the resources, in this case the battery charge during the scheduled time span. Finally, the bottom part shows a description of all the scheduled processes, which can be selected for further details.

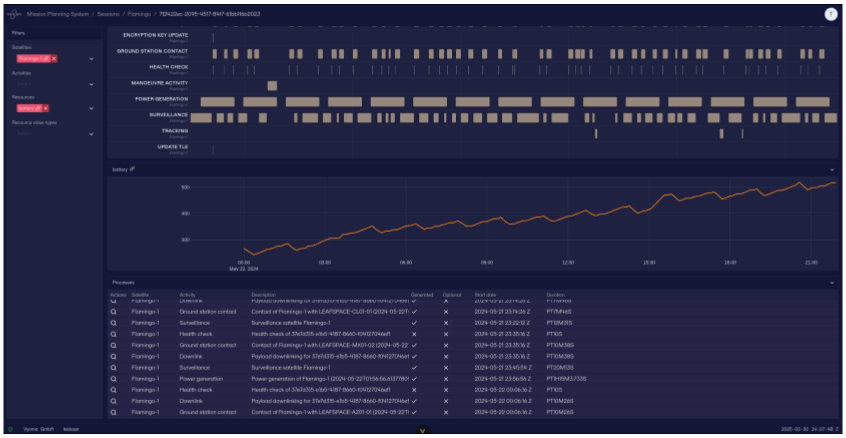

Fig. 12: Screenshot of Mission Planning System frontend.

6. Conclusions and discussion

In this paper, the architecture and the capabilities of Vyoma's Flight Dynamics System were presented. The tool is built upon the core functionalities of Orekit and extends them to fulfill the operational needs of Vyoma's pilot mission and future constellation. The FDS is modular with fundamental functionalities such as orbit propagation and event prediction that are complemented by separate and more specialised modules such as orbit determination, manoeuvre optimisation and conjunction assessment. Additional functionalities are being developed to further enhance Vyoma's FDS capabilities.

Several relevant test cases were presented to demonstrate the capabilities of the system. Fundamental functionalities such as orbit determination and manoeuvre calibration can be performed reliably and effectively to ensure the highest possible accuracy in the knowledge of the spacecraft state and of the assets that Vyoma's space-based sensors will observe. Since the safety of assets in space is Vyoma's first priority, the FDS collision avoidance capabilities were shown: using in-house state-of-the-art algorithms the FDS can reliably design collision avoidance manoeuvres in a matter of seconds while satisfying with various operational constraints. The presented test cases have also demonstrated that the optimisation techniques are scalable and adaptable to different problems such as station keeping applications, as well as orbit acquisition, and disposal.

Finally, the flight dynamics system can also be integrated with mission planning systems and other ground segments to support the operation of satellites and constellations. The ultimate goal of the developed FDS is to fully support automated satellite operations, starting with the Flamingo-1 pilot mission, and to expand its applicability to other systems.

Acknowledgements

This work is supported by the Joint Project Autonomous Satellite Operation (AUTOPS) within the funding line "Mobility" (Space sector) in accordance with the guidelines of the Bavarian Collaborative Research Program of the StMWi (BayVFP; Funding Reference Number: MRF-2307-0004) together with the consortium partners Vyoma GmbH (Consortium Leader), Technical University of Munich (TUM) – Chair of Pico- and Nanosatellites and Satellite Constellations, and the German Aerospace Center (DLR) – Mission Operations (RB-MIB).

References

[1] G. Janner, F. Strasser, E. Lerch, P. Silvagni, S. Frey, A flexible and extensible Mission Planning System applied to Space-Based Space Surveillance and Tracking, SpaceOps 2025, Montreal, Canada, May 26-30, 2025.

[2] L. Maisonobe, B. Cazabonne, R. Serra, E. Ward, M. Journot, S. Dinot, et al. CS-SI/Orekit: 12.2.1. 2024. DOI: 10.5281/zenodo.7249096.

[3] L. Maisonobe, P. Steitz, T. Neidhart, M. Diggory, E. Ward, et al. Hipparchus-Math/hipparchus: Hipparchus 3.0. 2023. DOI: 10.5281/zenodo.8418401.

[4] P. Cefola, J. San-Juan, S. Setty, and R. Proulx. Review of the Draper semi-analytical satellite theory (DSST). In *Proceedings of 18th Australian International Aerospace Congress*. January 2019.

[5] Vallado, D., Crawford, P., Hujsak, R., & Kelso, T. S. (2006, August). Revisiting spacetrack report# 3. In *AIAA/AAS astrodynamics specialist conference and exhibit* (p. 6753).

[6] J. M. Picone, A. E. Hedin, D. P. Drob, and A. C. Aikin. *NRLMSISE-00 empirical model of the atmosphere: Statistical comparisons and scientific issues.* Journal of Geophysical Research: Space Physics, 107(A12), 1468. 2002. DOI: 10.1029/2002JA009430.

[7] A. C. Morelli, Convex optimal control for on-board and on-ground low-thrust spacecraft guidance, PhD Thesis, 2023

[8] S. Bruinsma, D. Tamagnan, and R. Biancale. *The DTM-2000 empirical thermosphere model with new data assimilation and constraints at lower boundary: Accuracy and properties.* Journal of Atmospheric and Solar-Terrestrial Physics, 65(9), 1053-1070. 2003. DOI: 10.1016/S1364-6826(03)00137-8.

[9] Rauch, H. (1963). Solutions to the linear smoothing problem. *IEEE Transactions on Automatic Control*, *8*(4), 371–372. https://doi.org/10.1109/TAC.1963.1105600.

[10] S. Tanygin, Efficient Covariance Interpolation Using Blending Of Approximate State Error Transitions, *AAS/AIAA Astrodynamics Specialist Conference*, 2014.

[11] Consultative Committee for Space Data Systems (CCSDS). *Orbit Data Messages*. Blue Book. CCSDS 502.0-B-3. April 2023.

[12] J. van der Geer, J.A.J. Hanraads, R.A. Lupton, The art of writing a scientific article, J. Sci. Commun. 163. 2010. 51–59.

[13] Y.-W. Chang, J.-S. Chern, Ups and Downs of Space Tourism Development in 60 Years from Moon Register to SpaceShipTwo Crash, IAC-15-E4.2.8, 66th International Astronautical Congress, Jerusalem, Israel, 2015, 12 – 16 October.

[14] W. Strunk Jr., E.B. White, The Elements of Style, fourth ed., Longman, New York, 2000.

[15] S. Boyd, L. Vandenberghe, Convex Optimization, Cambridge University Press, 2004.

[16] K.S. Holkar, and L. M. Waghmare, "An overview of model predictive control," *International Journal of control and automation* 3.4, 47-63, 2010.

[17] D. Malyuta, T. P. Reynolds, M. Szmuk, T. Lew, R. Bonalli, M. Pavone, B. Açıkmeşe, Convex optimization for trajectory generation: A tutorial on generating dynamically feasible trajectories reliably and efficiently, IEEE Control Systems Magazine, Vol. 42.5, 2022.

[18] A. C. Morelli, C. Hofmann, F. Topputo, Robust Low-Thrust Trajectory Optimization Using Convex Programming and a Homotopic Approach, IEEE Transactions on Aerospace and Electronic Systems, Vol. 58.3, 2021.

[19] R. Armellin, Collision avoidance maneuver optimization with a multiple-impulse convex formulation, Acta Astronautica, Vol. 186, 2021.

[20] Y. Mao, M. Szmuk, B. Açıkmeşe, Successive convexification of non-convex optimal control problems and its convergence properties, 2016 IEEE 55th Conference on Decision and Control (CDC), Las Vegas, Nevada, 2016, 12–14 December.

[21] L. Blackmore, Autonomous precision landing of space rockets, Bridge, Vol. 4.46, 2016.

[22] C. Hofmann, A.C. Morelli, F. Topputo, Performance assessment of convex low-thrust trajectory optimization methods, Journal of Spacecraft and Rockets, Vol. 60.1, 2023.

[23]L. K. Newman, et al. Nasa conjunction assessment risk analysis updated requirements architecture. In: *AAS/AIAA Astrodynamics Specialist Conference*. 2019.

[24] A.C. Morelli, A. Morselli, C. Giordano, F. Topputo, Convex trajectory optimization using thrust regularization, Journal of Guidance, Control, and Dynamics, Vol. 47.2, 2024.

[25] F. Topputo, C. Zhang, Survey of Direct Transcription for Low-Thrust Space Trajectory Optimization with Applications, Abstract and Applied Analysis, Vol. 2014.1, 2014.

[26] A. Petropoulos, Low-thrust orbit transfers using candidate Lyapunov functions with a mechanism for coasting, AIAA/AAS Astrodynamics Specialist Conference and Exhibit, 16 August 2004.